*Inorg. Chem.* **2002**, *41*, 7143–7150


# Photoluminescence Switching of Azobenzene-Conjugated Pt(II) Terpyridine Complexes by Trans–Cis Photoisomerization

**Tomona Yutaka,[†,||] Ichiro Mori,[†] Masato Kurihara,[†] Jun Mizutani,[†] Naoto Tamai,[‡] Tsuyoshi Kawai,[§] Masahiro Irie,[§] and Hiroshi Nishihara*[,†]**

*Department of Chemistry, School of Science, The University of Tokyo, 7-3-1 Hongo, Bunkyo-ku, Tokyo 113-0033, Japan, Department of Chemistry, Faculty of Science, Kwansei Gakuin University, 2-1, Gakuen, Sanda, 669-1337 Japan, Department of Chemistry, Graduate School of Science and Technology, Kyushu University, and CREST, Japan Science and Technology Corporation, JST, 6-10-1 Hakozaki, Higashi-ku, Fukuoka 812-8581, Japan*

Received September 9, 2002

Pt(II) complexes with a terpyridylazobenzene ligand (tpyAB) were newly synthesized, and their photoluminescence properties by trans–cis isomerization of the azo moiety were investigated. In these complexes, upon excitation with 366-nm light in polar solvents such as DMF, DMSO, and propylene carbonate, trans-to-cis isomerization with significant UV–vis spectral changes occurred almost completely. Cis-to-trans isomerization was observed both by irradiation with visible light and by heat. The reduction peaks due to the terpyridine and the azo group in the cyclic voltammograms of the Pt complexes were shifted in the positive direction by trans-to-cis isomerization. Emission spectral changes due to trans–cis isomerization were observed for both the tpyAB and the Pt complexes. The significant differences in the emission properties of the complex compared to tpyAB include the observation that both the excitation and emission wavelengths were shifted to lower energy, located in the visible region. Moreover, the change in emission intensity between the trans and cis forms was more significant upon excitation with UV light, because the trans form of the complexes showed absolutely no emission. Accordingly, the azobenzene-conjugated Pt(II) terpyridine complexes promise to be doubly photofunctional materials, showing complete off–on switching of emission linked to the trans–cis conformation change.

## Introduction

Square-planar $d^8$ platinum(II) complexes containing the terpyridine ligand in solid or fluid solution are luminescent in the visible region with several emission modes due to intraligand $\pi-\pi^*$, MLCT, and intermolecular $\pi-\pi$ or Pt−Pt interactions.[1] There has been some effort to enhance their emission properties in solution, and it is known that $\pi$-accepting substituents (CN, etc.), $\pi$-donating substituents ($NR_2$, etc.), and conjugating groups (phenyl, naphthyl, etc.) at the 4′ position of the terpyridine ligand can extend emission lifetime dramatically.[1h,j,n] An intriguing subject of research in luminescent Pt terpyridine complexes would be the discovery of a means of switching the emission properties by some stimuli from the external field of new molecular-based devices. Azobenzene exhibits reversible trans−cis

* To whom correspondence should be addressed. E-mail: nisihara@chem.s.u-tokyo.ac.jp. Fax: +81-3-5841-8063. Phone: +81-3-5841-4346.
[†] University of Tokyo.
[‡] Kwansei Gakuin University.
[§] Kyushu University and CREST.
[||] E-mail: tomona@chem.s.u-tokyo.ac.jp.

(1) (a) Bailey, J. A.; Miskowski, V. M.; Gray, H. B. *Inorg. Chem.* **1993**, *32*, 369. (b) Yip, H.-K.; Cheng, L.-K.; Cheung, K.-K.; Che, C.-M. *J. Chem. Soc., Dalton Trans.* **1993**, 2933. (c) Aldrige, T. K.; Stacy, E. M.; McMillin, D. R. *Inorg. Chem.* **1994**, *33*, 722. (d) Akiba, M.; Umakoshi, K.; Sasaki, Y. *Chem. Lett.* **1995**, 607. (e) Bailey, J. A.; Hill, M. G.; Marsh, R. E.; Miskowski, V. M.; Schaefer, W. P.; Gray, H. B. *Inorg. Chem.* **1995**, *34*, 4591. (f) Büchner, R.; Field, J. S.; Haines, R.; Cunningham, C. T.; McMillin, D. *Inorg. Chem.* **1997**, *36*, 3952. (g) Arena, G.; Calogero, G.; Campagna, S.; Scolaro, L. M.; Ricevuto, V.; Romeo, R. *Inorg. Chem.* **1998**, *37*, 2763. (h) Crites, D. K.; Cunningham, C. T.; McMillin, D. R.; *Inorg. Chim. Acta* **1998**, *273*, 346. (i) Lai, S.-W.; Chan, M. C. W.; Cheung, K.-K.; Che, C.-M. *Inorg. Chem.* **1999**, *38*, 4262. (j) Büchner, R.; Cunningham, C. T.; Field, J. S.; Haines, R. J.; McMillin, D. R.; Summerton, G. C. *J. Chem. Soc., Dalton Trans.* **1999**, 711. (k) Tzeng, B.-C.; Fu, W.-F.; Che, C.-M.; Chao, H.-Y.; Cheung, K.-K.; Peng, S.-M. *J. Chem. Soc., Dalton Trans.* **1999**, 1017. (l) Michalec, J. F.; Bejune, S. A.; McMillin, D. R. *Inorg. Chem.* **2000**, *39*, 2708. (m) Hobert, S. E.; Carney, J. T.; Cummings, S. D. *Inorg. Chim. Acta* **2001**, *318*, 89. (n) Michalec, J. F.; Bejune, S. A.; Cuttell, D. G.; Summerton, G. C.; Gertenbach, J. A.; Field, J. S.; Haines, R. J.; McMillin, D. R. *Inorg. Chem.* **2001**, *40*, 2193.

10.1021/ic0260116 CCC: $22.00 
Published on Web 11/22/2002

**Chart 1**

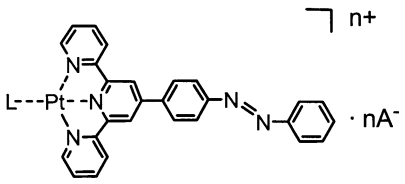


**PtL(tpyAB)·nA**

L = pyridine (py); Cl
$A^-$ = $PF_6^-$, $BPh_4^-$

isomerization by photoirradiation with UV and blue light, and its combination with transition metal complexes presents an intriguing system.[2] There have been some reports on fluorophores connected with azobenzenes,[3] but information on the cis isomer remains insufficient in most cases, primarily because of their instability. In our previous study,[4] the trans form of azobenzene-conjugated Ru(II) bis(terpyridine) complexes showed no emission. Moreover, these complexes did not exhibit trans-to-cis photoisomerization behavior because of the energy transfer from the $\pi-\pi^*$ excited state of the azobenzene unit to the MLCT state of the $Ru(tpy)_2$ unit. On the contrary, nonemissive Rh(III) complexes without intense MLCT or d−d bands in the visible region exhibited complete trans-to-cis photoisomerization.

In this study, we focused on the use of Pt(II) terpyridine complexes, as they emit more easily than the Ru(II) bis(terpyridine) complexes, and the Pt(II) terpyridine complexes possess weak MLCT bands in the region of higher energy (around 400 nm). These unique properties are likely to be advantageous for the material showing both emission and considerable trans-to-cis isomerization. The syntheses and photochemical and electrochemical properties of azobenzene-conjugated Pt(II) terpyridine complexes (PtL(tpyAB); Chart 1), in particular, their reversible trans−cis isomerization behavior and the complete switching of emission properties by trans−cis configuration changes, are described in this paper.

## Experimental Section

**Materials.** Dichloro(1,5-cyclooctadiene)platinum(II) (Pt(cod)$Cl_2$),[5] tpyAB,[4c] diiodo(1,5-cyclooctadiene)platinum(II) (Pt(cod)$I_2$),[6] dichlorobis(dimethyl sulfoxide)platinum(II) ([$PtCl_2(DMSO)_2$]),[7] and 2,2′:6′,2″-terpyridine (tpy)[8] were prepared according to the literature. [PtCl(tpy)]$PF_6$ (PtCl(tpy)·$PF_6$) was prepared by anion exchange from [PtCl(tpy)]Cl[9] using a saturated $NH_4PF_6$ aqueous solution. Potassium tetrachloroplatinate(II), ammonium hexafluorophosphate ($NH_4PF_6$), sodium tetraphenylborate ($NaBPh_4$), and pyridine (guaranteed grade), purchased from Kanto Chemicals, and silver trifluoromethanesulfonate ($AgCF_3SO_3$), purchased from Wako Pure Chemical Industries, were used as received. For the UV−vis absorption spectroscopy, dimethyl sulfoxide, propylene carbonate (guaranteed-grade, Kanto Chemicals), and *N*,*N*-dimethylformamide (spectroscopic grade, Dojin) were used as received. For the luminescence spectroscopy and the electrochemical measurements, *N*,*N*-dimethylformamide, methanol, and ethanol (HPLC grade, Kanto Chemicals) were used as received. Tetrabutylammonium tetrafluoroborate (lithium battery grade), used for the electrochemical measurements, was obtained from Tomiyama Chemicals.

**Apparatus.** UV−vis, $^1$H NMR, and ESI MS spectra were recorded with Jasco V-570 and Hewlett-Packard 8453 UV−vis spectrometers, JEOL EX270 and Bruker AM 500 spectrometers, and a Micromass LCT (time-of-flight mass spectrometer), respectively. Photoisomerization measurements were carried out under a nitrogen atmosphere using a 500 W super high-pressure mercury lamp USH-500D (USHIO) (for trans-to-cis photoisomerization) or a 500 W xenon lamp UXL-500D-O (USHIO) (for cis-to-trans photoisomerization) as an irradiation source. The 366-nm light was isolated with a Toshiba UV-D35 glass filter. Visible light ($\lambda >$ 430 nm) was isolated with a Toshiba Y-43 glass filter. Emission spectra were measured in a quartz tube (8 mm$\phi$) with an F-4500 fluorescence spectrophotometer (Hitachi). Emission spectra at 77 K were measured in the quartz tube, placed in a liquid nitrogen Dewar flask equipped with quartz windows. The transient fluorescence spectra were measured with a gated streak-scope system (Hamamatsu Photonics, C4334-01, C5094, and C4792). The excitation light source was a $N_2$ laser (Hamamatsu Photonics, LN-203), the excitation laser power, pulse width, and wavelength of which were 0.1 mJ, 600 ps, and 337.1 nm, respectively. The sample solution was placed in a liquid nitrogen-filled Cryostat (Oxford Instruments, DN1704) with quartz windows.

**Crystal Structure Determination.** All measurements were made on a Rigaku Mercury with graphite monochromated Mo K$\alpha$ radiation ($\lambda$ = 0.71070 Å), and the data were collected and processed using CrystalClear (Rigaku).

Pt(py)(tpyAB)·$2BPh_4$ was crystallized as orange-red blocks by slow diffusion from diethyl ether into an acetonitrile solution. A crystal of Pt(py)(tpyAB)·$2BPh_4$ with the approximate dimensions of 0.4 × 0.4 × 0.4 mm$^3$ was mounted on a glass loop. The data were collected to a maximum $2\theta$ value of 55.0°. The linear absorption coefficient, $\mu$, for Mo K$\alpha$ radiation is 22.5 cm$^{-1}$. An empirical absorption correction was applied, which resulted in transmission factors ranging from 0.329 to 1.025. The structure was solved by direct methods (SIR92)[10] and was expanded using Fourier techniques.[11] The structure was refined by full-matrix least-squares refinement[12] on *F*. All non-hydrogen atoms were refined anisotropically.

PtCl(tpyAB)·$PF_6$ was crystallized as orange-red blocks by slow diffusion from diethyl ether into a *N*,*N*-dimethylacetamide (DMA)

(2) (a) Rau, H. In *Photochromism. Molecules and Systems*; Dürr, H. B., Laurent, H., Eds.; Elsevier: Amsterdam, 1990; p 165. (b) Anzai, J.; Osa, T. *Tetrahedron* **1994**, *50*, 4039.
(3) (a) Zacharias, P. S.; Ameerunisha, S.; Korupoju, S. R. *J. Chem. Soc., Perkin Trans. 2* **1998**, 2055. (b) Yam, V. W.-W.; Lau, V. C.-Y.; Wu, L.-X. *J. Chem. Soc., Dalton Trans.* **1998**, 1461. (c) Tsuchiya, S. *J. Am. Chem. Soc.* **1999**, *121*, 48.
(4) (a) Yutaka, T.; Kurihara, M.; Nishihara, H. *Mol. Cryst. Liq. Cryst.* **2000**, *343*, 193. (b) Yutaka, T.; Kurihara, M.; Kubo, K.; Nishihara, H. *Inorg. Chem.* **2000**, *39*, 3438. (c)Yutaka, T.; Mori, I.; Kurihara, M.; Mizutani, J.; Kubo, K.; Furusho, S.; Matsumura, K.; Tamai, N.; Nishihara, H. *Inorg. Chem.* **2001**, *40*, 4986.
(5) McDermott, J. X.; White, J. F.; Whitesides, G. M. *J. Am. Chem. Soc.* **1976**, *98*, 6521.
(6) Clark, H. C.; Manzer, L. E. *J. Organomet. Chem.* **1973**, *59*, 411.
(7) Kitching, W.; Moore, C. J.; Doddrell, D. *Inorg. Chem.* **1970**, *9*, 541.
(8) Jameson, D. L.; Guise, L. E. *Tetrahedron Lett.* **1991**, *32*, 1999.
(9) (a) Howe-Grant, M.; Lippard, S. J. *Inorg. Synth.* **1980**, *20*, 101. (b) Annibale, G.; Brandoliso, M.; Piteteri, B. *Polyhedron* **1995**, *14*, 451.
(10) *SIR92*: Altomare, A.; Cascarano, G.; Giacovazzo, C.; Guagliardi, A.; Burla, M.; Polidori, G.; Camalli, M. *J. Appl. Crystallogr.* **1994**, *27*, 435.
(11) *DIRDIF99*: Beurskens, P. T.; Admiraal, G.; Beurskens, G.; Bosman, W. P.; de Gelder, R.; Israel, R.; Smits, J. M. M. *The DIRDIF-99 program system*; Technical Report of the Crystallography Laboratory; University of Nijmegen: The Netherlands, 1999.
(12) Least squares function minimized: $\sum w(|F_o| - |F_c|)^2$ where $w$ = least squares weights.

**Table 1.** Crystal Data and Structure Refinement for Pt(py)(tpyAB)·2$PF_6$ and PtCl(tpyAB)·$PF_6$·DMA

| | Pt(py)(tpyAB)·2$BPh_4$ | PtCl(tpyAB)·$PF_6$·DMA |
|---|---|---|
| empirical formula | $C_{80}H_{64}N_6B_2Pt$ | $C_{35}H_{37}N_7ClF_6O_2PPt$ |
| fw | 1326.14 | 963.23 |
| cryst dimens ($mm^3$) | 0.40 × 0.40 × 0.40 | 0.3 × 0.3 × 0.2 |
| cryst syst | triclinic | triclinic |
| *a* (Å) | 10.932(2) | 7.13(5) |
| *b* (Å) | 11.586(3) | 16.28(2) |
| *c* (Å) | 25.709(13) | 17.06(3) |
| α (°) | 93.119(11) | 113.45(3) |
| *β* (°) | 95.885(5) | 91.95(1) |
| *γ* (°) | 100.354(2) | 92.37(2) |
| *V* ($Å^3$) | 3177.5(16) | 1813.1(89) |
| space group | $P\bar{1}$ | $P\bar{1}$ |
| *Z* | 2 | 2 |
| $D_{calcd}$ ($g/cm^3$) | 1.386 | 1.764 |
| $F_{000}$ | 1348.00 | 952.00 |
| no. measured total reflns | 17888 | 14387 |
| no. measured unique reflns | 10158 | 7888 |
| no. observations | 8031 ($I > 1.5\sigma(I)$) | 6416 ($I > 3\sigma(I)$) |
| no. variables | 781 | 218 |
| residuals *R*;[a] $R_w$[b] | 0.104; 0.148 | 0.081; 0.093 |
| GOF[c] | 3.63 | 3.89 |
| max peak in final diff. map ($e^-/Å^3$) | 2.25 | 1.54 |
| min peak in final diff. map ($e^-/Å^3$) | −3.54 | −1.07 |

[a] $R = \sum||F_o| - |F_c||/\sum|F_o|$. [b] $R_w = [\sum w(|F_o| - |F_c|)^2/\sum w|F_o|^2]^{1/2}$. [c] GOF $= [\sum w(|F_o| - |F_c|)^2/(N_o - N_v)^2]^{1/2}$, where $N_o$ = number of observations and $N_v$ = number of variables.

solution. A crystal of PtCl(tpyAB)·$PF_6$·DMA with the approximate dimensions of 0.3 × 0.3 × 0.2 $mm^3$ was mounted on a glass loop. The data were collected to a maximum $2\theta$ value of 54.9°. The linear absorption coefficient, $\mu$, for Mo Kα radiation is 40.5 $cm^{-1}$. The structure was solved by Patterson methods (SHELX97)[13] and expanded using Fourier techniques.[11] The structure was refined by full-matrix least-squares refinement[12] on *F*. The Pt atom was refined anisotropically, but other lighter atoms were refined isotropically because the position of the phenyl group was not settled enough to define anisotropically. The crystal data and structure refinement for Pt(py)(tpyAB)·2$PF_6$ and PtCl(tpyAB)·$PF_6$·DMA are summarized in Table 1.

**Femtosecond Transient Absorption Spectra.** The arrangement for the femtosecond pump−probe experiment was essentially the same as that reported elsewhere.[14] Briefly, the laser system consisted of a hybridly mode-locked, dispersion-compensated femtosecond dye laser (Coherent, Satori 774) and a dye amplifier (Continuum, RGA 60−10 and PTA 60). The dye laser (gain dye Pyridine 2 and saturable absorber DDI) was pumped with a cw mode-locked Nd:YAG laser (Coherent, Antares 76S). The sample was excited by the second harmonic (360 nm) of the fundamental (center wavelength 720 nm, pulse width ∼200 fs fwhm) at a repetition rate of 10 Hz. The residual portion of the fundamental output was focused on a 1-cm $H_2O$ cell to generate a femtosecond supercontinuum probe pulse. The planes of polarization of the pump and probe beams were set to the magic angle (54.7°) to avoid any anisotropic contribution to the transient signal. Both the beams were focused on the sample in a 2-mm cuvette at an angle of less than 5°. Transient spectra were obtained by averaging over 200 pulses and analyzed by an intensified multichannel detector (Princeton Instruments, ICCD-576) as a function of the probe delay time. The spectra were corrected for the intensity variations and time dispersions of the supercontinuum. Rise and decay curves at a fixed wavelength were measured with a photodiode−monochromator (Japan Spectroscopic, CT-10) combination. The concentration of the sample for transient absorption spectra was kept within $1-1.5 \times 10^{-4}$ M. The solution was allowed to flow through a 2-mm flow cell using a magnetically coupled gear pump (Micropump, 040-332) to avoid any possibility of sample damage during the transient absorption measurement.

**Measurements of Trans−Cis Isomerization and Quantum Yields.** A 1-cm light path length quartz cell was used for the photoisomerization measurements. The concentration of the samples was around $1 \times 10^{-5}$ M, and the sample solution was degassed by $N_2$ bubbling before photoirradiation, and stirred during trans-to-cis and cis-to-trans isomerization. The cis-to-trans thermal isomerization rate was measured by the "kinetic" mode of Hewlett-Packard 8453 UV−vis spectrometers, where the UV−vis spectra were measured continuously with determined intervals, at a given constant temperature. Quantum yields of trans-to-cis photoisomerization were measured for each complex by using $K_3[Fe(C_2O_4)_3]$ as a chemical actinometer, from the absorbance changes within 10% trans-to-cis structural conversion.

**Electrochemical Measurements.** A glassy carbon rod (diameter 5 mm; Tokai Carbon GC-20) was embedded in Pyrex glass, and the cross section was used as a working electrode. Cyclic voltammetry measurements were carried out in a standard one-compartment cell under Ar gas, equipped with a platinum wire counter electrode and a $Ag/Ag^+$ reference electrode with a BAS CV-50W voltammetric analyzer.

**Measurements of Emission Spectra.** All of the samples were measured in EtOH−MeOH−DMF (EMD) glass (5:5:1 (v/v)) at 77 K. As the time course measurement of emission spectra, the trans-to-cis isomerization reaction of the sample was carried out by photoirradiation with 366-nm light in pure DMF, and the emission spectra were measured after dilution with a mixture of EtOH−MeOH (1:1 (v/v)).

**Syntheses. General Synthetic Procedure for [Pt(py)(tpyAB)]-$X_2$ (Pt(py)(tpyAB)·2X) ($X^- = PF_6^-$ or $BPh_4^-$).** To a suspension of Pt(cod)$I_2$ (0.10 g, 0.18 mmol) in *N*,*N*-dimethylacetamide (5 mL) was added $AgCF_3SO_3$ (0.10 g, 0.40 mmol). The resulting mixture was stirred at room temperature for 5 min. The AgI precipitate was filtered through a Celite layer. TpyAB (0.058 g, 0.090 mmol) was added to the filtrate, and the solution was stirred for 30 min at room temperature. The solution was filtered off and treated with pyridine (15 $\mu$L). The solution was then stirred for 3 min and filtered, and excess $NH_4PF_6$ or $NaBPh_4$ in water was added. The precipitate was filtered off and recrystallized from acetonitrile−ether to yield orange powders.

**[PtCl(tpyAB)]$PF_6$ (PtCl(tpyAB)·$PF_6$).** To a solution of [$PtCl_2$-$(DMSO)_2$] (0.048 g, 0.11 mmol) in DMSO (5 mL) was added dropwise $AgCF_3SO_3$ (0.029 g, 0.11 mmol) in DMSO (2 mL). The reaction mixture was heated under reflux for 16 h at 100 °C, and the precipitated AgCl was removed by filtration. The filtrate was heated at 100 °C, and tpyAB (0.047 g, 0.11 mmol) was added. The mixture was refluxed for 3 h and filtered through a Celite layer. An excess amount of $NH_4PF_6$ in water was added to the solution. The precipitate was filtered off and recrystallized from acetonitrile−ether to yield orange powders: yield 0.062 g (69%). Anal. Calcd for $C_{27}H_{19}N_5ClF_6PPt·1/2H_2O$: C, 40.64; H, 2.53; N, 8.78. Found: C, 40.62; H, 2.81; N, 8.46. $^1H$ NMR (DMF-$d_7$): $\delta$ 9.33 (s, 2H), 9.18 (d, 2H, $J$ = 5.3 Hz), 9.07 (d, 2H, $J$ = 8.0 Hz), 8.73 (t, 2H, $J$ = 8.1 Hz), 8.56 (d, 2H, $J$ = 9.5 Hz), 8.23 (d, 2H, $J$ = 9.1 Hz), 8.18 (t, 2H, $J$ = 8.1 Hz), 8.1−7.9 (2H, this signal overlapped with

(13) *SHELX97*: Sheldrick, G. M.; Schneider, T. R. *Methods Enzymol.* **1997**, *277*, 319.
(14) (a) Tamai, N.; Masuhara, H. *Chem. Phys. Lett.* **1992**, *191*, 189. (b) Mitra, S.; Tamai, N. *Chem. Phys. Lett.* **1998**, *282*, 391.

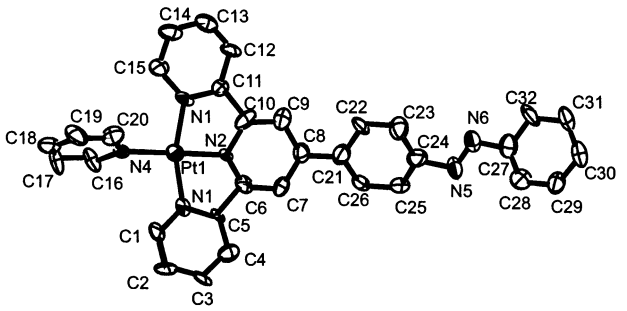


**Figure 1.** ORTEP diagram of Pt(py)(tpyAB)·2$BPh_4$ with 50% probability. H atoms and $BPh_4^-$ ions have been omitted for clarity. Selected bond lengths (Å), bond angles (deg), and torsion angles (deg) are as follows: Pt(1)−N(1) 2.003(13), Pt(1)−N(2) 1.923(13), Pt(1)−N(3) 2.018(12), Pt(1)−N(4) 2.015(13), N(5)−N(6) 1.29(2), N(1)−Pt(1)−N(2) 80.0(5), N(2)−Pt(1)−N(3) 81.4(6), N(1)−Pt(1)−N(4) 99.2(5), N(3)−Pt(1)−N(4) 99.3(5), N(5)−N(6)−C(27)−C(28) −28.3(37), N(5)−N(6)−C(27)−C(32) 155.4(23), C(7)−C(8)−C(21)−C(22) −143.1(24), C(7)−C(8)−C(21)−C(26) 30.6(38), C(9)−C(8)−C(21)−C(22) 30.4(38), C(9)−C(8)−C(21)−C(26) −155.8(26), N(1)−C(5)−C(6)−N(2) 0.2(27), N(2)−C(10)−C(11)−N(3) 0.6(26).

that of DMF, the solvent peak), 7.70 (m, 3H). ESI MS *m*/*z* 644.10 ($[PtCl(tpyAB)]^+$ requires 644.10).

The cis form was prepared by photoirradiation to *trans*-PtCl(tpyAB). $^1$H NMR (DMF-$d_7$): $\delta$ 9.13 (d, 2H, $J$ = 5.8 Hz), 9.03 (s, 2H), 8.99 (d, 2H, $J$ = 8.4 Hz), 8.65 (t, 2H, $J$ = 9.2 Hz), 8.20 (d, 2H, $J$ = 8.5 Hz), 8.10 (m, 2H, $J$ = 8.5 Hz), 7.69 (m, 2H), 7.32 (t, 2H, $J$ = 9.2 Hz), 7.24 (d, 2H, $J$ = 8.9 Hz), 7.08 (t, 1H, $J$ = 7.9 Hz).

## Results and Discussion

**Syntheses and Characterization.** $[PtCl(tpyAB)]PF_6$ was prepared by a one-pot reaction of $PtCl_2(DMSO)_2$ with tpyAB. $[Pt(py)(tpyAB)]^{2+}$ complexes with $PF_6^-$ and $BPh_4^-$ were synthesized according to the literature,[15] using Pt(cod)$I_2$, in which 1,5-cyclooctadiene acted as a very strong translabilizing ligand, and was used as the starting material. All of the Pt complexes were characterized by $^1$H NMR, UV−vis, and ESI MS spectra and elemental analysis. As Pt(py)(tpyAB)·2$BPh_4$ and PtCl(tpyAB)·2$PF_6$, X-ray crystallographic analysis was achieved. An ORTEP image of the Pt(py)(tpyAB)·2$BPh_4$ is shown in Figure 1 with selected bond distances and bond angles. The coordination geometry of the Pt atom was square planar but was distorted because of the restricted bite angle of the tridentate tpyAB ligand. The structure of the Pt terpyridine complex unit was similar to that of previously reported complexes,[16] and the Pt−N bond length and N−Pt−N bond angles were in good agreement with those of previously reported Pt terpyridine complexes.[1] The ancillary pyridine ligand was nearly perpendicular to the terpyridine plane (the torsion angle, N(3)−Pt(1)−N(4)−C(20) was −69.4(23)°) because of the steric repulsion between the H atoms of the ancillary pyridine ligand attached to C(16) and C(20), and also because of the steric hindrance of the H atoms of the terpyridine ligand attached to C(15) and C(1). Two phenyl rings of the azobenzene unit were twisted around the azo group by 43.8°, a value which was calculated from the torsion angles of N(6)−N(5)−C(24)−C(23) and N(5)−N(6)−C(27)−C(28). The torsion angles of C(7)−C(8)−C(21)−C(26) and C(9)−C(8)−C(21)−C(22) were 30.6° and 30.4°, respectively, which indicated that the phenyl ring attached to the terpyridine and the central pyridine ring of the terpyridine were not coplanar. Because of the existence of the large counterion $BPh_4^-$, each molecule was isolated, as suggested by the intermolecular Pt−Pt distance (10.9(32) Å).

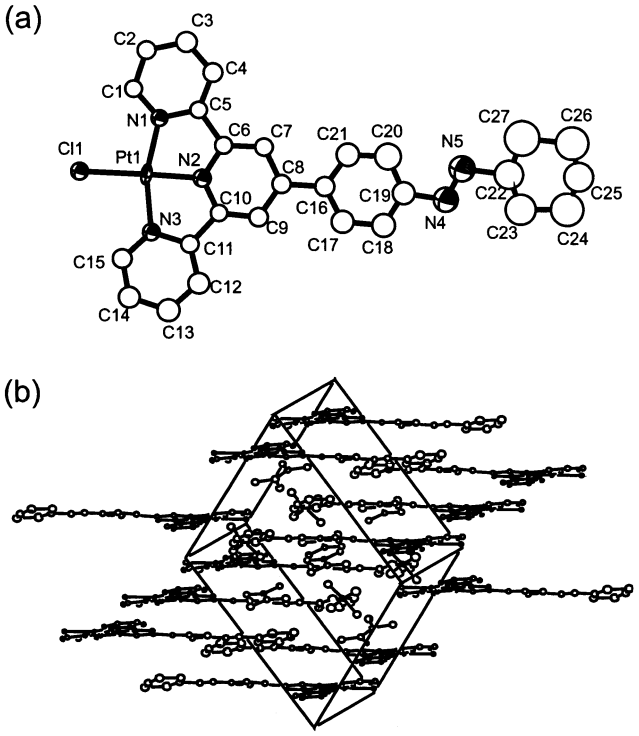


**Figure 2.** (a) ORTEP diagram of PtCl(tpyAB)·$PF_6$·DMA with 50% probability. H atoms, $PF_6^-$ ions, and DMA have been omitted for clarity. Selected bond lengths (Å), bond angles (deg), and torsion angles (deg) are as follows: Pt(1)−Cl(1) 2.289(11), Pt(1)−N(1) 2.006(10), Pt(1)−N(2) 1.911(13), Pt(1)−N(3) 2.010(11), N(4)−N(5) 1.21(2), Cl(1)−Pt(1)−N(1) 100.3(5), Cl(1)−Pt(1)−N(2) 178.7(3), N(1)−Pt(1)−N(2) 81.0(4), Cl(1)−Pt(1)−N(3) 97.3(3), C(7)−C(8)−C(16)−C(17) 172.6(19), C(9)−C(8)−C(16)−C(17) −5.0(32), C(19)−N(4)−N(5)−C(22) 179.8(23), N(5)−N(4)−C(19)−C(20) 0.8(37), N(4)−N(5)−C(22)−C(27) −169.7(45). (b) Crystal packing of PtCl(tpyAB)·$PF_6$·DMA.

The X-ray crystallographic structure of PtCl(tpyAB)·$PF_6$ is shown in Figure 2a with selected bond distances and angles. The difference in the structure of this complex from that of Pt(py)(tpyAB)·2$BPh_4$ is that all of the phenyl rings of both azobenzene and terpyridine were almost coplanar. It should be mentioned that the geometry in the crystal may not be the same as that in solution because the potential energy required for twisting the parent biphenyl is very small, and thus, the dihedral angles in biphenyl-containing crystals readily adapt so as to optimize the crystal packing. The crystal lattice consisted of parallel sheets of cations and anions, as shown in Figure 2b, indicating that there may have been weak $\pi-\pi$ interactions between the cations.

The UV−vis absorption spectra of Pt(py)(tpyAB)·2$PF_6$, tpyAB, and Pt(py)(tpy)·2$PF_6$ are shown in Figure 3, inset. As Pt(py)(tpy)·2$PF_6$, two MLCT bands were observed at 367

(15) Lowe. G.; Vilaivan, T. *J. Chem. Res., Synop.* **1996**, 386.
(16) (a) Bailey, J.; Gray, H. *Acta Crystallogr.* **1992**, *C48*, 1420. (b) Bailey, J. A.; Catalano, V. J.; Gray, H. B. *Acta Crystallogr.* **1993**, *C49*, 1598. (c) Roszak, A. W.; Clement, O.; Buncel, E. *Acta Crystallogr.* **1996**, *C52*, 1645. (d) Lowe, G.; Ross, S. A.; Probert, M.; Cowley, A. *J. Chem. Soc., Chem. Commun*. **2001**, 1288.

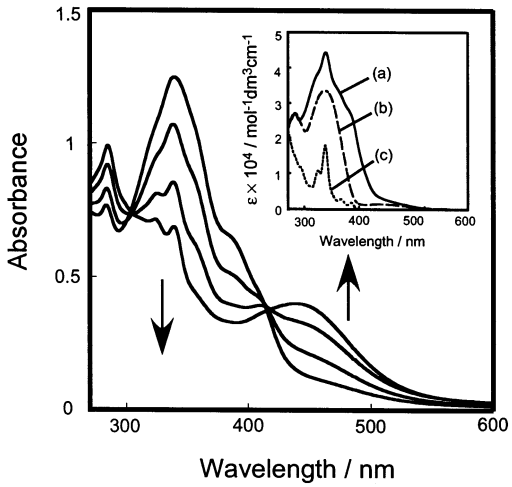


**Figure 3.** UV−vis spectral change of Pt(py)(tpyAB)·$2PF_6$ in propylene carbonate ($3.0 \times 10^{-5}$ M) upon irradiation at 366 nm for 50 min. Inset: UV−vis absorption spectra of (a) Pt(py)(tpyAB)·$2PF_6$, (b) tpyAB, and (c) Pt(py)(tpy)·$2PF_6$.

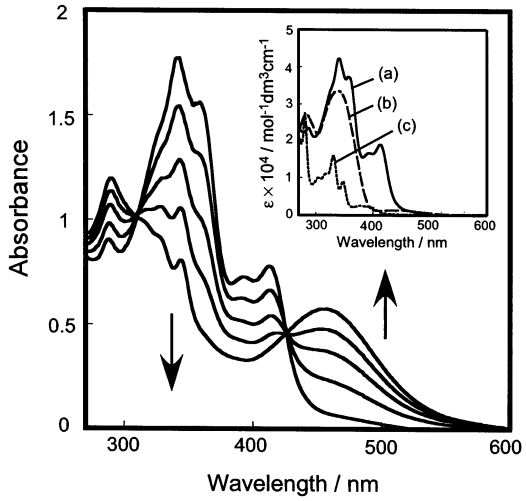


**Figure 4.** UV−vis spectral change of PtCl(tpyAB)·$PF_6$ in DMF ($4.2 \times 10^{-5}$ M) upon irradiation at 366 nm for 25 min. Inset: UV−vis absorption spectra of (a) PtCl(tpyAB)·$PF_6$, (b) tpyAB, and (c) PtCl(tpy)·$PF_6$.

and 386 nm, and LC bands appeared at shorter wavelengths. The spectrum of Pt(py)(tpyAB)·$2PF_6$ was interpreted by the superposition of the spectra of tpyAB and Pt(py)(tpy)·$2PF_6$, while the azo $\pi-\pi^*$ band was broadened and red-shifted by ca. 10 nm. UV−vis absorption spectra of PtCl(tpyAB)·$PF_6$, tpyAB, and PtCl(tpy)·$PF_6$ are shown in Figure 4, inset. PtCl(tpy)·$PF_6$ had a broad MLCT band at 370−420 nm, and many LC bands at the shorter wavelength region, and its azo $\pi-\pi^*$ band was broader and more red-shifted (20 nm) than those observed in Pt(py)(tpyAB)·$2PF_6$. The molar extinction coefficient, $\epsilon$, of the MLCT band was around $2 \times 10^4$ $M^{-1}$ $cm^{-1}$, a value which was significantly larger than that of Pt(py)(tpy)·$2PF_6$. This indicated that the $\pi$-conjugation between the azobenzene unit and the Pt terpyridine complex unit of PtCl(tpyAB)·$PF_6$ was stronger than that in Pt(py)(tpyAB)·$2PF_6$.

**Trans-to-Cis Photoisomerization Behavior.** UV−vis spectral changes of Pt(py)(tpyAB)·$2PF_6$ and PtCl(tpyAB)·$PF_6$ upon irradiation with 366-nm light are shown in Figures 3 and 4, respectively. The absorbance of the azo $\pi-\pi^*$ transition band decreased, and that of the azo n$-\pi^*$ transition band increased. These results indicated that trans-to-cis photoisomerization of the Pt complexes did occur. Pt(py)(tpyAB)·$2BPh_4$ shows a spectral change very similar to that of Pt(py)(tpyAB)·$2PF_6$. The cis form revealed an intensive band at around 450 nm for Pt(py)(tpyAB)·$2PF_6$ and Pt(py)(tpyAB)·$2BPh_4$, and around 470 nm for PtCl(tpyAB)·$PF_6$. These bands were assigned to azo n$-\pi^*$ bands, but as extremely intense bands, similar to those of the Rh(III) complexes. Trans-to-cis photoisomerization behavior was supported by $^1$H NMR, IR, and transient absorption spectroscopy. The $^1$H NMR spectral change of PtCl(tpyAB)·$PF_6$ (dilute solution, $10^{-4}$ M) by photoirradiation was monitored in DMF-$d_7$ (see Experimental Section). Most of the signals were shifted to the higher magnetic field, and this phenomenon was identical to that of the Rh(III) complexes. Pt(py)(tpyAB)·$2BPh_4$ was able to isomerize even in a KBr pellet, and, in the IR spectrum, cis −N═N− stretching appeared at 1530 $cm^{-1}$.

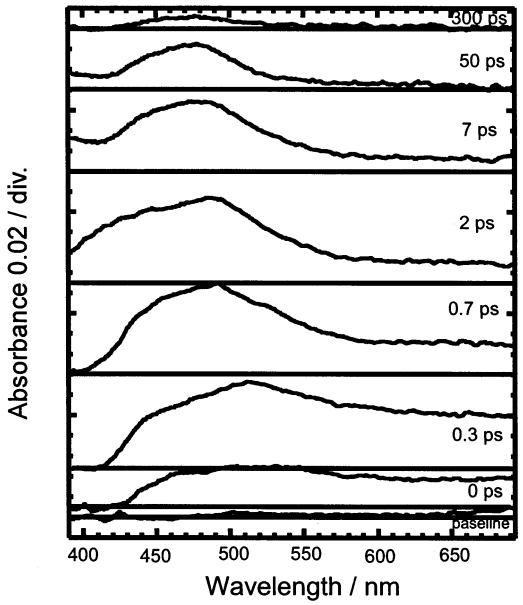


**Figure 5.** Time-resolved transient absorption spectra of Pt(py)(tpyAB)·$2PF_6$ in acetonitrile, excited by 360-nm light.

Figure 5 shows the transient absorption spectra of Pt(py)(tpyAB)·$2PF_6$ in acetonitrile. At first, a broad $S_n \leftarrow S_2$ absorption band appeared at ∼500 nm, and then an intense $S_n \leftarrow S_1$ absorption band at ∼450 nm appeared. The lifetimes of the $S_2$ and $S_1$ states were 1.6 and 3.1 ps, respectively. The behavior was similar to that of organic azobenzenes and the Rh(III) complexes.

Trans-to-cis photoisomerization was observed in several solvents, for example, acetonitrile, *N*, *N*-dimethylformamide (DMF), dimethyl sulfoxide (DMSO), and propylene carbonate (PC). The quantum yields ($\Phi_{t\rightarrow c}$) are listed in Table 2. $\Phi_{t\rightarrow c}$ in acetonitrile was much smaller than in other solvents; this tendency was similar to that of the Rh(III) complexes. $\Phi_{t\rightarrow c}$ of Pt(py)(tpyAB)·$2PF_6$ depended upon the solvent. $\Phi_{t\rightarrow c}$ was found to be in the following order: DMF > DMSO > PC, thus indicating that a more polar solvent afforded a smaller quantum yield. As Pt(py)(tpyAB)·$2BPh_4$ and PtCl-

**Table 2.** Trans-to-Cis Photoisomerization Quantum Yields ($\Phi_{t\rightarrow c}$) of the Pt Complexes

| solvent | dielectric constant $\epsilon$[a] | $10^3\Phi_{t\rightarrow c}$ Pt(py)(tpyAB)·2$PF_6$ | Pt(py)(tpyAB)·2$BPh_4$ | PtCl(tpyAB)·$PF_6$ |
|---|---|---|---|---|
| DMF | 38.3 | 1.8 | 1.5 | 1.6 |
| DMSO | 47.2 | 0.77 | 1.6 | 1.1 |
| PC | 68.8 | 0.33 | 0.80 | 1.1 |

[a] Lide, D. R. *CRC Handbook of Chemistry and Physics*, 79th ed.; CRC Press: Boca Raton, FL, 1998.

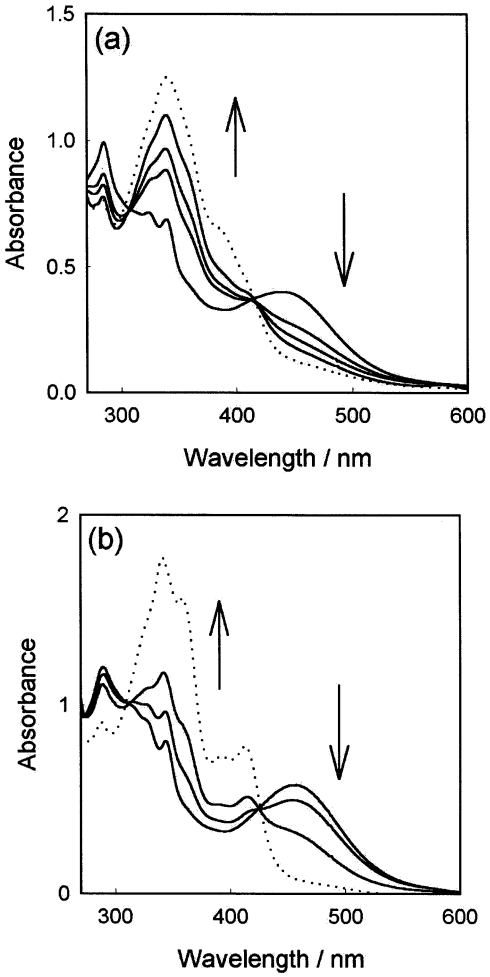


**Figure 6.** (a) UV−vis spectral change of Pt(py)(tpyAB)·2$PF_6$ in PC by heating the solution at 100 °C for 12 h and (b) UV−vis spectral change of PtCl(tpyAB)·$PF_6$ in DMF upon irradiation with visible light ($\lambda$ > 430 nm) for 5 h. The dotted line indicates the pure trans form.

(tpyAB)·$PF_6$, the solvent effects were not significant. In DMSO and PC, the quantum yields of the $BPh_4^-$ salts were higher than those of the $PF_6^-$ salts. These counterion effects were similar to those of the Rh(III) complexes,[4] but the variation of $\Phi_{t\rightarrow c}$ was not wide especially in the case of PtCl(tpyAB)·$PF_6$, with less charge of the complex cations than the $[Pt(py)(tpyAB)]^{2+}$ complexes and the Rh(III) complexes.

**Cis-to-trans Isomerization Behavior.** Figure 6a shows the UV−vis spectral changes of Pt(py)(tpyAB)·2$PF_6$ in PC upon heating to 100 °C, and Figure 6b shows the UV−vis spectral changes of PtCl(tpyAB)·$PF_6$ in DMF upon irradiation with visible light (>430 nm). All of the Pt complexes exhibited cis-to-trans isomerization upon heating the solution

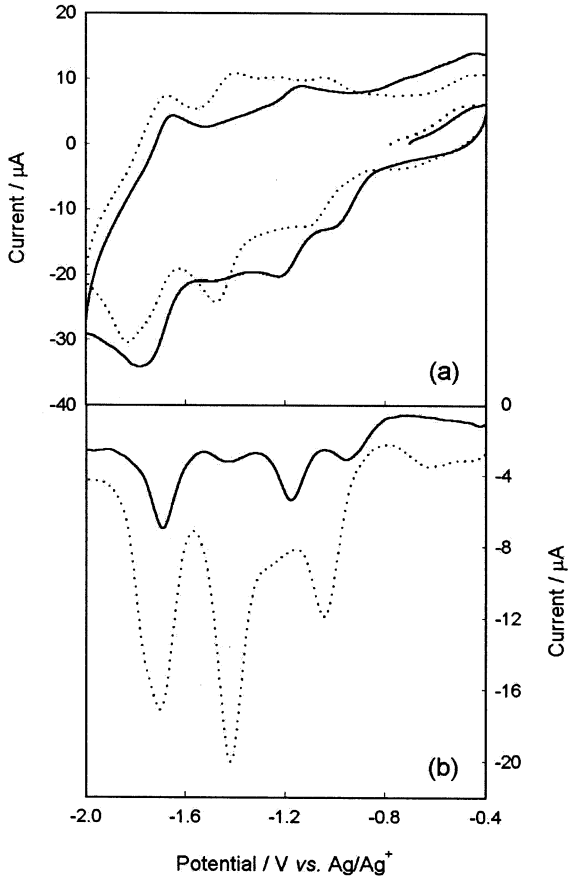


**Figure 7.** (a) Cyclic voltammograms and (b) differential pulse voltammograms of *trans*-PtCl(tpyAB)·$PF_6$ (···) and *cis*-PtCl(tpyAB)·$PF_6$ (—) in 0.1 M $Bu_4NBF_4$−DMF.

in the dark or by irradiation with visible light, and 50−80% of the trans form was recovered in DMF, PC, and DMSO. There are two possible reasons for the incomplete recovery of the trans form by visible light irradiation; the one is reaching a photostationary state, and the other is occurrence of photodegradation. The former cannot be denied because the photochemical pathway is not simple in a complex for which visible absorption would be mixing of azo n−$\pi$* and MLCT bands. However, the degradation must be significant because even thermal isomerization cannot attain the complete trans form.

**Electrochemistry.** Cyclic voltammograms and differential pulse voltammograms of *trans*- and *cis*-PtCl(tpyAB)·$PF_6$ are shown in Figure 7. Comparison with the redox behavior of PtCl(tpy)·$PF_6$ with reversible peaks at −1.13 and −1.69 V suggested that the two reversible peaks due to the terpyridine ligand were shifted in the negative direction by 300 mV, as a result of the presence of the electron-withdrawing azo group. As PtCl(tpyAB)·$PF_6$, reduction of the azo group was observed at −1.10 V. In the cis form, the reduction potentials of both the azo group and the terpyridine ligand were shifted in the positive direction by 100 and 300 mV, respectively, from those of the trans form. These positive shifts of the reduction potentials indicated that the terpyridine $\pi$* level and the azo $\pi$* level of the cis form were both lower than those of the trans form. This finding was further supported by the UV−vis absorption spectra, which suggested that the

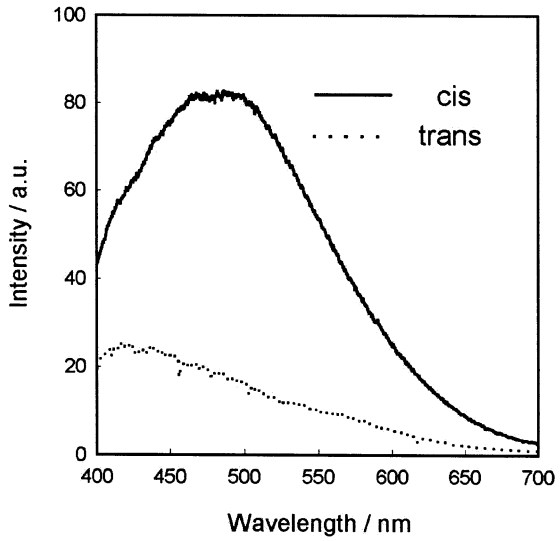


**Figure 8.** Emission spectral change of tpyAB ligand in EtOH−MeOH−DMF = 5:5:1 (v/v) at 77 K upon irradiation with 366-nm light for 1 min. The excitation wavelength was 300 nm.

azo n−$\pi$* state was able to interact with the azo $\pi-\pi$* and MLCT (d(Pt)−$\pi$*(terpyridine)) states, and that the absorption band of the azo n−$\pi$* transition had shifted to lower energy.

Cyclic voltammograms of Pt(py)(tpyAB) also showed a similar effect of redox potential shift, but these voltammograms were more complicated than those of PtCl(tpyAB), most likely because the coordination of the pyridine ligand was weak and unstable against electrochemical stimulation.

**Emission Properties.** Before the detailed discussion of the 2D emission spectra of azobenzene-conjugated Pt terpyridine complexes, the emission properties of the tpyAB ligand should be discussed. Figure 8 shows the emission spectra of *trans*- and *cis*-tpyAB in EMD glass at 77 K. Although weak emission was observed even in the trans form, the emission intensity increased in the cis form. This enhanced emission, compared with the emission spectrum of 2,2′:6′,2″-terpyridine ligand,[17] was attributed to the terpyridine $^3\pi-\pi$* state.

As for the Pt complexes employed in this study, emission at room temperature was not observed. Figure 9 shows the contour line plots of the excitation−emission spectra of *trans*- and *cis*-Pt(py)(tpyAB)·2$PF_6$ in an EMD glass at 77 K. There was no significant peak in the trans form (Figure 9a), but four sharp peaks were observed at 325 nm (excitation)/480 nm (emission), 375 nm/480 nm, 300 nm/600 nm, and 450 nm/600 nm (Figure 9b). Two interpretations of the enhancement of emission in the cis form were suggested. Because of the nonplanar geometry of the cis form, as well as the reduced $\pi$-conjugation effect, (1) photoinduced electron transfer from the nitrogen lone pair to the emissive unit was inhibited,[3a] and/or (2) the triplet state energy of the azo chromophore was higher than that of the trans form and thus inhibited the nonradiative deactivation pathway from MLCT excited states to the azo $\pi-\pi$* state.[3b]

Figure 10 shows the emission spectral changes of Pt(py)(tpyAB)·2$PF_6$ by trans-to-cis photoisomerization excited at 337 nm (a) and at 450 nm (b). Pt(py)(tpyAB)·2$BPh_4$ and

(17) Sarkar, A.; Chakravorti, S. *J. Lumin.* **1995**, *63*, 143.

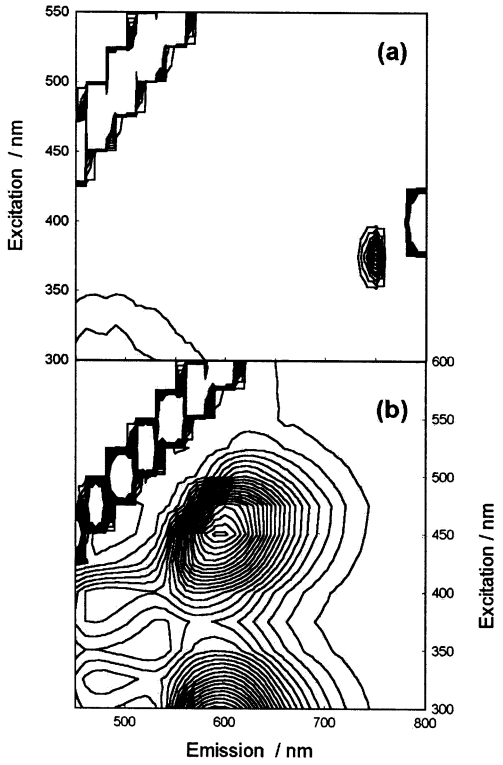


**Figure 9.** Excitation−emission contour plot of (a) *trans*-Pt(py)(tpyAB)·2$PF_6$ and (b) *cis*-Pt(py)(tpyAB)·2$PF_6$ in EtOH−MeOH−DMF = 5:5:1 (v/v) at 77 K.

PtCl(tpyAB)·$PF_6$ exhibited similar behavior to that of Pt(py)(tpyAB)·2$PF_6$, and the intensity of emission increased as the proportion of the cis form increased. By 337-nm excitation, two emission maxima were observed at 460 and 600 nm in the cis form, and they were assigned to the emission from the ligand $^3\pi-\pi$* and $^3$MLCT states, respectively, on the basis of previous studies of the emission spectra of Pt(II) terpyridine complexes.[1] This assignment was supported by the excitation spectra and the lifetime measurements (vide infra). The excitation spectrum of emission at 600 nm was very similar to the UV−vis spectrum of the cis form (Figure 3), and thus, the emission at 600 nm mainly originated because of 450-nm excitation. Moreover, this band represented the azo n−$\pi$* transition, as interacted with the azo $\pi-\pi$* and the Pt MLCT band. The excitation spectrum of emission at 460 nm indicated that the origin was a band at around 380 nm. This band could be considered as the ligand or as an azo $\pi-\pi$* band. Emission lifetimes were measured to be 2 ns for 460 nm, and 40 $\mu$s for 600 nm, respectively. This result supported the preceding assignment of the emission spectral peaks, and the lifetime of the emission at 600 nm was comparable to that of Pt(py)(4′-phenyl-tpy)·2$PF_6$. The emission spectrum of Pt(py)(4′-phenyl-tpy)·2$PF_6$ excited at 337 nm was similar to that of the other Pt(II) terpyridine complexes. The emission lifetime at 600 nm was 41 $\mu$s. It is suggested by the present findings that *cis*-Pt(py)(tpyAB)·2$PF_6$ emits from a Pt(py)(4′-phenyl-tpy)·2$PF_6$ unit and, furthermore, that there is no $\pi$-conjugation effect beyond the azo group. In the trans form, there was a very weak emission from the ligand $^3\pi-\pi$* state by 337-nm excitation, and there was no emission by 450-nm

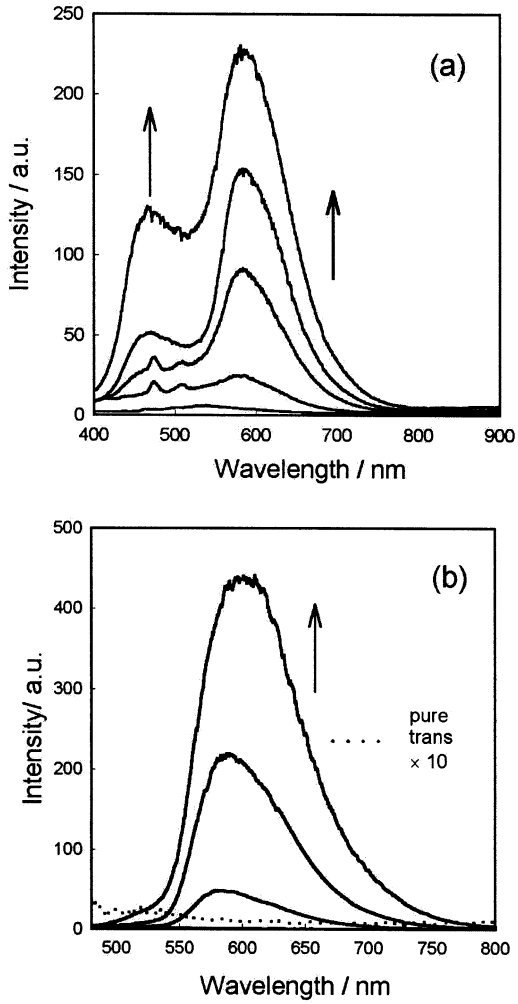


**Figure 10.** Emission spectral changes of Pt(py)(tpyAB)·2$PF_6$ in EtOH−MeOH−DMF = 5:5:1 (v/v) at 77 K upon irradiation with 366-nm light for 8 min. The excitation wavelength was (a) 337 nm and (b) 450 nm.

excitation. The former weak emission would have originated from an intense absorbance comprising the superposition of the ligand $\pi-\pi^*$ and the azo $\pi-\pi^*$ transition at 337 nm. As the latter case, it would be reasonable to assume no emission had occurred, because there was only a very weak absorbance due to a forbidden azo $n-\pi^*$ transition in the UV−vis spectrum of the trans form at 450 nm (Figure 3).

There are two significant facts regarding emission properties of the Pt complexes. First, the excitation wavelength was shifted by 150 nm to lower energy, compared with that of free ligand. As for the tpyAB ligand, the excitation wavelength was in the high-energy region at 300 nm, which was suitable for the emission of 2,2′:6′,2″-terpyridine and *cis*-tpyAB, as indicated by the 3D excitation−emission contour plot, in which case, even the trans form emitted slightly. Second, the trans form revealed absolutely no emission at 600 nm; that is, off−on switching of emission could be achieved by trans−cis isomerization. In our previous study on azobenzene-conjugated Ru(II) bis(terpyridine) complexes, the $Ru(tpy)_2$ unit should be emissive in the cis form; however, the Ru complexes did not provide adequate photoswitching materials, because the trans-to-cis photoisomerization was not sufficiently observed. Accordingly, azobenzene-conjugated Pt(II) terpyridine complexes were shown to be promising multifunctional materials, because trans−cis conformation change in these complexes is linked with emission spectral change.

**Acknowledgment.** This work was supported by Grants-in-Aid for scientific research (Nos. 13022212, 14050032, and 14204066) from the Ministry of Education, Science, Sports and Culture, Japan, the Tokyo Ohka Foundation, and the Hayashi Memorial Foundation for Female Natural Scientists.

**Supporting Information Available:** Synthetic and characterization data of Pt complexes; X-ray crystallographic data of Pt(py)(tpyAB)·2$PF_6$ and PtCl(tpyAB)·$PF_6$·DMA in CIF format. This material is available free of charge via the Internet at http://pubs.acs.org.

IC0260116